VISUAL COGNITION, 2009, 17 (6/7), 945–978

Psychology Press
Taylor & Francis Group

# Modelling search for people in 900 scenes: A combined source model of eye guidance

Krista A. Ehinger and Barbara Hidalgo-Sotelo

*Department of Brain and Cognitive Sciences, Massachusetts Institute of Technology, Cambridge, MA, USA*

Antonio Torralba

*Computer Science and Artificial Intelligence Laboratory, and Department of Electrical Engineering and Computer Science, Massachusetts Institute of Technology, Cambridge, MA, USA*

Aude Oliva

*Department of Brain and Cognitive Sciences, Massachusetts Institute of Technology, Cambridge, MA, USA*



How predictable are human eye movements during search in real world scenes? We recorded 14 observers' eye movements as they performed a search task (person detection) in 912 outdoor scenes. Observers were highly consistent in the regions fixated during search, even when the target was absent from the scene. These eye movements were used to evaluate computational models of search guidance from three sources: saliency, target features, and scene context. Each of these models independently outperformed a cross-image control in predicting human fixations. Models that combined sources of guidance ultimately predicted 94% of human agreement, with the scene context component providing the most explanatory power. None of the models, however, could reach the precision and fidelity of an attentional map defined by human fixations. This work puts forth a benchmark for computational models of search in real world scenes. Further improvements in

Please address all correspondence to Aude Oliva, Department of Brain and Cognitive Sciences, Massachusetts Institute of Technology, Cambridge, MA, USA. E-mail: oliva@mit.edu

KAE and BH-S contributed equally to the work. The authors would like to thank two anonymous reviewers and Benjamin Tatler for their helpful and insightful comments on an earlier version of this manuscript. KAE was partly funded by a Singleton graduate research fellowship and by a graduate fellowship from an Integrative Training Program in Vision grant (T32 EY013935). BH-S was funded by a National Science Foundation Graduate Research Fellowship. This work was also funded by an NSF CAREER award (0546262) and a NSF contract (0705677) to AO, as well as an NSF CAREER award to AT (0747120). Supplementary information available on the following website: http://cvcl.mit.edu/SearchModels


http://www.psypress.com/viscog DOI: 10.1080/13506280902834720

modelling should capture mechanisms underlying the selectivity of observers' fixations during search.

***Key words:*** Computational model; Contextual guidance; Eye movement; Real world scene; Saliency; Target feature; Visual search



Daily human activities involve a preponderance of visually guided actions, requiring observers to determine the presence and location of particular objects. How predictable are human search fixations? Can we model the mechanisms that guide visual search? Here, we present a dataset of 45,144 fixations recorded while observers searched 912 real world scenes and evaluate the extent to which search behaviour is (1) consistent across individuals and (2) predicted by computational models of visual search guidance.

Studies of free viewing have found that the regions selected for fixation vary greatly across observers (Andrews & Coppola, 1999; Einhauser, Rutishauser, & Koch, 2008; Parkhurst & Neibur, 2003; Tatler, Baddeley, & Vincent, 2006). However, the effect of behavioural goals on eye movement control has been known since the classic demonstrations by Buswell (1935) and Yarbus (1967) showing that observers' patterns of gaze depended critically on the task. Likewise, a central result emerging from studies of oculomotor behaviour during ecological tasks (driving, e.g., Land & Lee, 1994; food preparation, e.g., Hayhoe, Shrivastava, Mruczek, & Pelz, 2003; sports, e.g., Land & McLeod, 2000) is the functional relation of gaze to one's momentary information processing needs (Hayhoe & Ballard, 2005).

In general, specifying a goal can serve as a referent for interpreting internal computations that occur during task execution. Visual search—locating a given target in the environment—is an example of a behavioural goal which produces consistent patterns of eye movements across observers. Figure 1 (later) shows typical fixation patterns of observers searching for pedestrians in natural images. Different observers often fixate remarkably consistent scene regions, suggesting that it is possible to identify reliable, strategic mechanisms underlying visual search and to create computational models that predict human eye fixations.

Various mechanisms have been proposed which may contribute to attention guidance during visual search. Guidance by statistically unexpected, or salient, regions of a natural image has been explored in depth in both modelling and behavioural work (e.g., Bruce & Tsotsos, 2006; Itti, Koch, & Niebur, 1998; Koch & Ullman, 1985; Li, 2002; Rosenholtz, 1999; Torralba, 2003a). Numerous studies have shown that regions where the local statistics differ from the background statistics are more likely to attract an observer's gaze. Distinctive colour, motion, orientation, or size constitute the

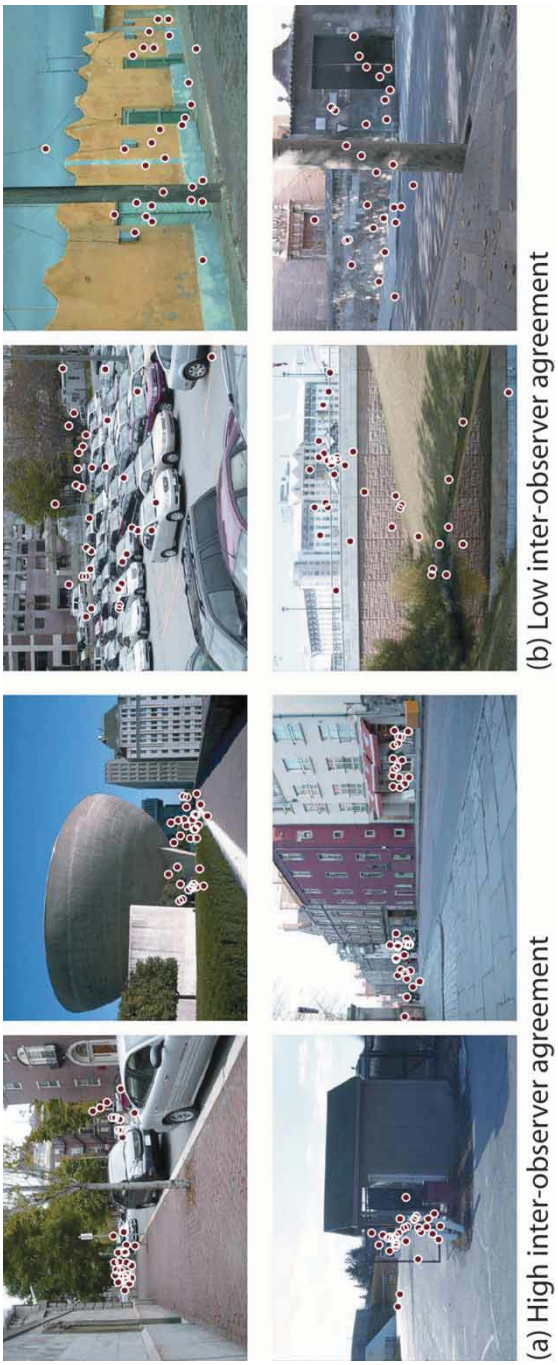


**Figure 1.** Examples of target-absent scenes with (a) high and (b) low inter-observer agreement. Dots represent the first three fixations from each observer. To view this figure in colour, please see the online issue of the Journal.

most common *salient* attributes, at least in simple displays (for a review, Wolfe & Horowitz, 2004). Guidance by saliency may also contribute to early fixations on complex images (Bruce & Tsotsos, 2006; Harel, Koch, & Perona, 2006; Itti & Koch, 2000; Parkhurst, Law, & Niebur, 2002; van Zoest, Donk, & Theeuwes, 2004), particularly when the scene context is not informative (Parkhurst et al., 2002; Peters, Iyer, Itti, & Koch, 2005) or during free viewing. In natural images, it is interesting to note that objects are typically more salient than their background (Elazary & Itti, 2008; Torralba, Oliva, Castelhano, & Henderson, 2006), so oculomotor guidance processes may use saliency as a heuristic to fixate objects in the scene rather than the background.

In addition to bottom-up guidance by saliency, there is a top-down component to visual attention that is modulated by task. During search, observers can selectively attend to the scene regions most likely to contain the target. In classical search tasks, target features are an ubiquitous source of guidance (Treisman & Gelade, 1980; Wolfe, 1994, 2007; Wolfe, Cave, & Franzel, 1998; Zelinsky, 2008). For example, when observers search for a red target, attention is rapidly deployed towards red objects in the scene. Although a natural object, such as a pedestrian, has no single defining feature, it still has statistically reliable properties (upright form, round head, straight body) that could be selected by visual attention. In fact, there is considerable evidence for target-driven attentional guidance in real world search tasks (Einhauser et al., 2008; Pomplun, 2006; Rao, Zelinsky, Hayhoe, & Ballard, 2002; Rodriguez-Sanchez, Simine, & Tsotsos, 2007; Tsotsos et al., 1995; Zelinsky, 2008).

Another top-down component which applies in ecological search tasks is scene context. Statistical regularities of natural scenes provide rich cues to target location and appearance (Eckstein, Drescher & Shimozaki, 2006; Hoiem, Efros, & Hebert, 2006; Oliva & Torralba, 2007; Torralba & Oliva, 2002, 2003). Within a glance, global information can provide useful information about spatial layout and scene category (Greene & Oliva, 2009; Joubert, Rousselet, Fize, & Fabre-Thorpe, 2007; McCotter, Gosselin, Sowden, & Schyns, 2005; Renninger & Malik, 2004; Rousselet, Joubert, & Fabre-Thorpe, 2005; Schyns & Oliva, 1994). Categorical scene information informs a viewer of which objects are likely to be in the scene and where (Bar, 2004; Biederman, Mezzanotte, & Rabinowitz, 1982; de Graef, Christiaens, & d'Ydewalle, 1990; Friedman, 1979; Henderson, Weeks, & Hollingworth, 1999; Loftus & Mackworth, 1978). Furthermore, global features can be extracted quickly enough to influence early search mechanisms and fixations (Castelhano & Henderson, 2007; Chaumon, Drouet, & Tallon-Baudry, 2008; Neider & Zelinky, 2006; Torralba et al., 2006; Zelinsky & Schmidt, this issue 2009).

In the present work, we recorded eye movements as observers searched for a target object (a person) in over 900 natural scenes and evaluated the predictive value of several computational models of search. The purpose of this modelling effort was to study *search guidance*, that is, where observers look while deciding whether a scene contains a target. We modelled three sources of guidance: bottom-up visual saliency, learned visual features of the target's appearance, and a learned relationship between target location and scene context. The informativeness of these models, individually and combined, was assessed by comparing the regions selected by each model to human search fixations, particularly in target-absent scenes (which provide the most straightforward and rigorous comparison).

The diversity and size of our dataset (14 observers' fixations on 912 urban scenes)[1] provides a challenge for computational models of attentional guidance in real world scenes. Intelligent search behaviour requires an understanding of scenes, objects and the relationships between them. Although humans perform this task intuitively and efficiently, modelling visual search is challenging from a computational viewpoint. The combined model presented here achieves 94% of human agreement on our database; however, a comprehensive understanding of human search guidance will benefit from mutual interest by cognitive and computer vision scientists alike.



## EXPERIMENTAL METHOD

### Participants

Fourteen observers (18–40 years old, with normal acuity) were paid for their participation ($15/hour). They gave informed consent and passed the eyetracking calibration test.

### Apparatus

Eye movements were recorded at 240 Hz using an ISCAN RK-464 video-based eyetracker. Observers sat at 75 cm from the display monitor, 65 cm from the eyetracking camera, with their head centred and stabilized in a headrest. The position of the right eye was tracked and viewing conditions were binocular. Stimuli were presented on a 21-inch CRT monitor with a resolution of $1024 \times 768$ pixels and a refresh rate of 100 Hz. Presentation of the stimuli was controlled with Matlab and Psychophysics Toolbox (Brainard, 1997; Pelli, 1997). The following calibration procedure was

[1] The complete dataset and analysis tools will be made available at the authors' website.

performed at the beginning of the experiment and repeated following breaks. Participants sequentially fixated five static targets positioned at 0° (centre) and at 10° of eccentricity. Subsequently, the accuracy of the calibration was tested at each of nine locations evenly distributed across the screen, including the five calibrated locations plus four targets at $+/-5.25°$ horizontally and vertically from centre. Estimated fixation position had to be within 0.75° of visual angle for all nine points, otherwise the experiment halted and the observer was recalibrated.

## Stimuli

The scenes consisted of 912 colour pictures of urban environments, half containing a pedestrian (target present) and half without (target absent). Images were of resolution $800 \times 600$ pixels, subtending $23.5 \times 17.7$ ° of visual angle. When present, pedestrians subtended on average $0.9 \times 1.8°$ (corresponding to roughly $31 \times 64$ pixels). For the target-present images, targets were spatially distributed across the image periphery (target locations ranged from 2.7 ° to 13 ° from the screen centre; median eccentricity was 8.6°), and were located in each quadrant of the screen with approximately equal frequency.[2]

## Procedure

Participants were instructed to decide as quickly as possible whether a person was present in the scene. Responses were registered via the keyboard, which terminated the image presentation. Reaction time and eye movements were recorded. The first block consisted of the same 48 images for all participants, and was used as a practice block to verify that the eye could be tracked accurately. The experiment was composed of 19 blocks of 48 trials each and 50% target prevalence within each block. Eyetracking calibration was checked after each block to ensure tracking accuracy within 0.75° of each calibration target. Each participant performed 912 experimental trials, resulting in an experiment duration of 1 hour.

## Eye movement analysis

Fixations were identified on smoothed eye position data, averaging the raw data over a moving window of eight data points (33 ms). Beginning and end

[2] See additional figures on authors' website for distribution of targets and fixations across all images in the database.

positions of saccades were detected using an algorithm implementing an acceleration criterion (Araujo, Kowler, & Pavel, 2001). Specifically, the velocity was calculated for two overlapping 17 ms intervals; the onset of the second interval was 4.17 ms after the first. The acceleration threshold was a velocity change of 6°/s between the two intervals. Saccade onset was defined as the time when acceleration exceeded threshold and the saccade terminated when acceleration dropped below threshold. Fixations were defined as the periods between successive saccades. Saccades occurring within 50 ms of each other were considered to be continuous.

## HUMAN EYE MOVEMENTS RESULT

### Accuracy and eye movement statistics



On average, participants' correct responses when the target was present (hits) was 87%. The false alarm rate (fa) in target-absent scenes was 3%. On correct trials, observers' mean reaction time was 1050 ms (1 standard error of the mean or SEM = 18) for target-present and 1517 ms (1 SEM = 14) for target-absent. Observers made an average of 3.5 fixations (excluding the initial central fixation but including fixations on the target) in target-present scenes and 5.1 fixations in target-absent scenes. The duration of "search fixations" exclusively (i.e., exploratory fixations excluding initial central fixation and those landing on the target) averaged 147 ms on target-present trials and 225 ms on target-absent trials. Observers spent an average of 428 ms fixating the target-person in the image before indicating a response.

We focused our modelling efforts on predicting locations of the first *three* fixations in each scene (but very similar results were obtained when we included all fixations). We introduce next the measures used to compare search model's predictions and humans' fixations.

### Agreement among observers

How much eye movement variability exists when different observers look at the same image and perform the same task? First, we computed the regularity, or agreement among locations fixated by separate observers (Mannan, Ruddock, & Wooding, 1995; Tatler, Baddeley, & Gilchrist, 2005). As in Torralba et al. (2006), a measure of inter-observer agreement was obtained for each image by using the fixations generated by all-except-one observers. The "observer-defined" image region was created by assigning a value of 1 to each fixated pixel and 0 to all other pixels, then applying a Gaussian blur (cutoff frequency = 8 cycles per image, about 1° visual angle). The observer-defined region was then used to predict fixations of the

excluded observer. For each image, this process was iterated for all observers. Thus, this measure reflected how consistently different observers selected similar regions to fixate. Figure 1 shows examples of target-absent scenes with high and low values of inter-observer agreement.

Not all of the agreement between observers is driven by the image, however—human fixations exhibit regularities that distinguish them from randomly selected image locations. Tatler and Vincent (this issue 2009) present compelling evidence that robust oculomotor biases constrain fixation selection independently of visual information or task (see also Tatler, 2007). Qualitatively, we observe in our dataset that the corners of the image and the top and bottom edges were less frequently fixated than regions near the image centre. We therefore derived a measure to quantify the proportion of inter-observer agreement that was independent of the particular scene's content (see also Foulsham & Underwood, 2008; Henderson, Brockmole, Castelhano, & Mack, 2007). Our "cross-image control" was obtained using the procedure described previously, with the variation that the observer-defined region for one image was used to predict the excluded observer's fixations from a *different* image selected at random.

The Receiver Operating Characteristic (ROC) curves for inter-observer agreement and the cross-image control are shown in Figure 2. These curves show the proportion of fixations that fall within the fixation-defined map (detection rate) in relation to the proportion of the image area selected by the map (false alarm rate). In the following, we report the area under the curve (AUC), which corresponds to the probability that the model will rank an actual fixation location more highly than a nonfixated location, with a value ranging from .5 (chance performance) to 1 (perfect performance) (Harel et al., 2006; Renninger, Verghese, & Coughlan 2007; Tatler et al., 2005).

The results in Figure 2 show a high degree of inter-observer agreement, indicating high consistency in the regions fixated by different observers for both target-absent scenes (AUC = .93) and target-present scenes (AUC = .95). Overall, inter-observer agreement was higher in target-present than in target-absent scenes, $t(805) = 11.6$, $p < .0001$, most likely because fixating the target was the primary goal of the search. These agreement curves represent an upper bound for comparing performance of the computational models with human fixations. Furthermore, the cross-image control produced an AUC of .68 and .62 for target-absent and target-present scenes respectively (random chance: AUC = .5). The cross-image control line represents the proportion of human agreement due to oculomotor biases and other biases in the stimuli set, and serves as the lower bound on the performance of the models.

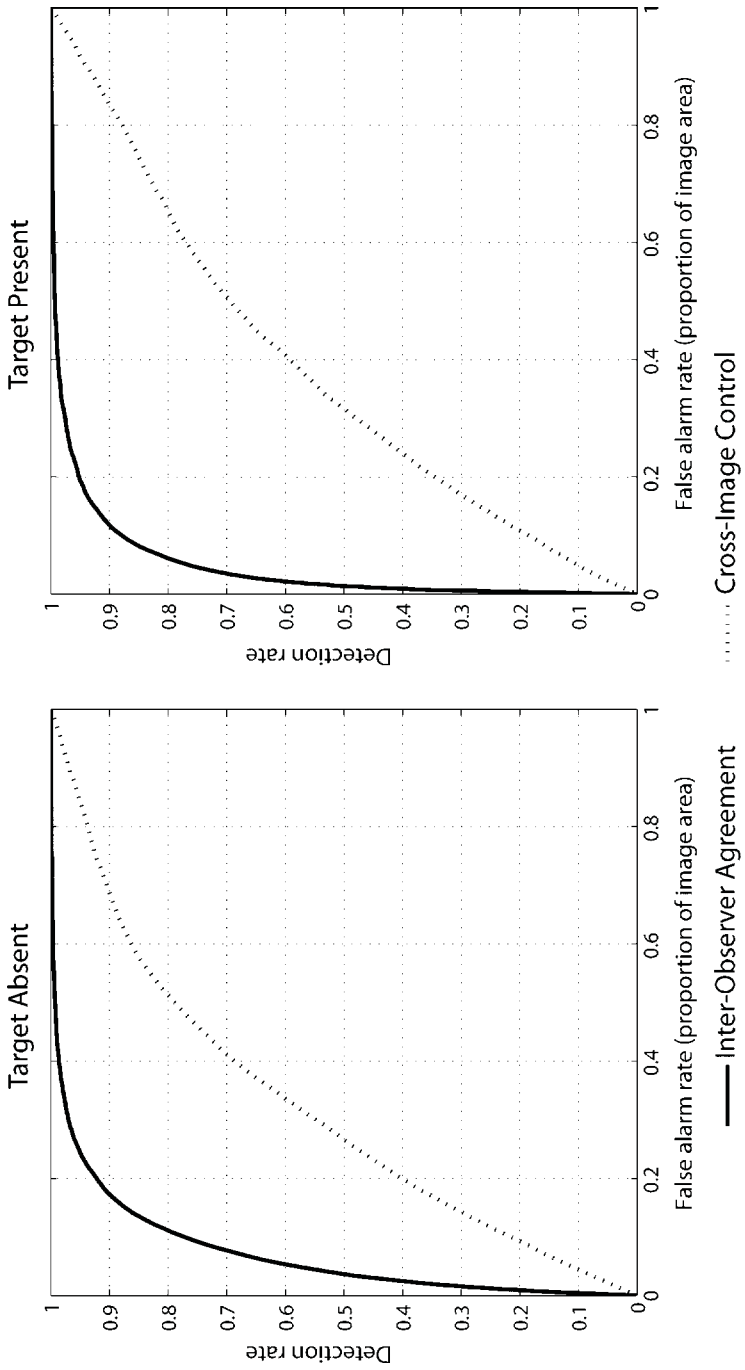


**Figure 2.** Inter-observer agreement and cross-image control for target-absent (left) and target-present (right) scenes. The false alarm rate, on the x-axis, corresponds to the proportion of the image selected by the model.

## MODELLING METHODS

Here we used the framework of visual search guidance from Torralba (2003b) and Torralba et al. (2006). In this framework, the attentional map (M), which will be used to predict the locations fixated by human observers, is computed by combining three sources of information: Image saliency at each location ($M_S$), a model of guidance by target features ($M_T$), and a model of guidance by the scene context ($M_C$).

$$M(x, y) = M_S(x, y)^{\gamma 1}\ M_T(x, y)^{\gamma 2}\ M_C(x, y)^{\gamma 3} \quad (1)$$

The exponents ($\gamma 1$, $\gamma 2$, $\gamma 3$), which will act like weights if we take the logarithm of Equation 1, are constants that are required when combining distributions with high-dimensional inputs that were independently trained, to ensure that the combined distribution is not dominated by one source (the procedure for selecting the exponents is described later). Together, these three components ($M_S$, $M_T$, and $M_C$) make up the combined attentional map (M).

Figure 3 illustrates a scene with its corresponding saliency, target features, and scene context maps, as well as a combined map integrating the three sources of guidance. Each model makes predictions, represented as a surface map, of the regions that are likely to be fixated. The best model should capture as many fixations as possible within as finely constrained a region as possible. In the following sections, we evaluate the performance of each of the three models individually, followed by a model combining sources of attentional guidance.

### Guidance by saliency

Computational models of saliency are generally based on one principle: They use a mixture of local image features (e.g., colour and orientation at various spatial scales) to determine regions that are local outliers given the statistical distribution of features across a larger region of the image. The hypothesis underlying these models is that locations whose properties differ from neighbouring regions or the image as a whole are the most informative. Indeed, rare image features in an image are more likely to be diagnostic of objects (Elazary & Itti, 2008; Torralba et al., 2006), whereas repetitive image features or large homogenous regions are unlikely to be object-like (Bravo & Farid, 2006; Rosenholtz, Li, & Nakano, 2007).

Computing saliency involves estimating the distribution of local features in the image. Here we used the statistical saliency model described in Torralba et al. (2006), including the use of an independent validation set to determine an appropriate value for the exponent.[3] The independent

[3] In our validation set, the best exponent for the saliency map was .025, which is within the optimal range of .01–.3 found by Torralba et al. (2006).

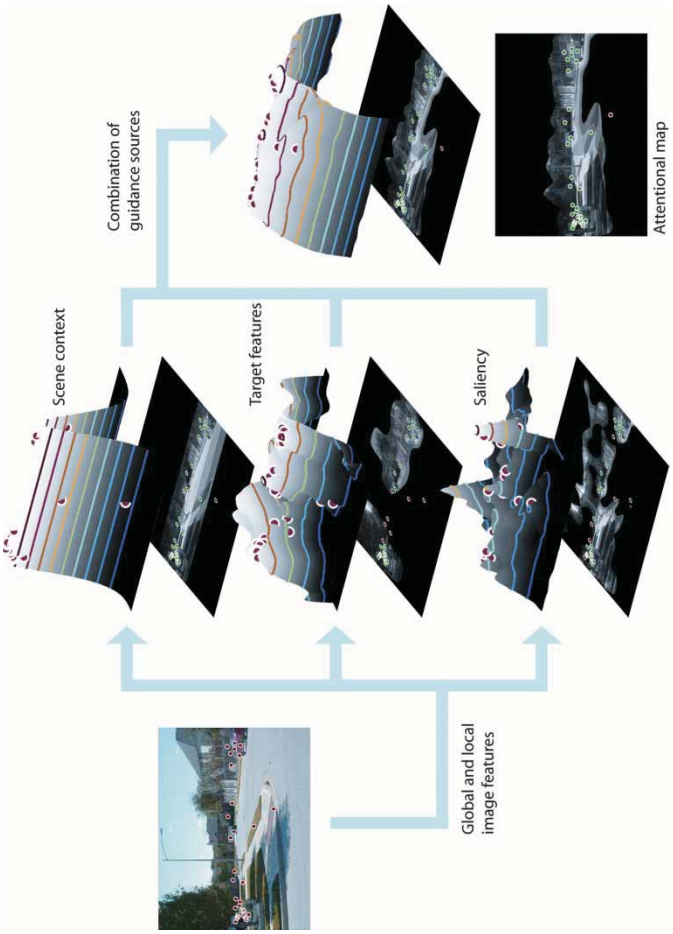


**Figure 3.** Illustration of a target-present image from the dataset, with the computational maps for three sources of guidance, and the combined attentional map. The flattened maps show the image regions selected when the model is thresholded at 30% of the image. To view this figure in colour, please see the online issue of the Journal.

validation set was composed of 50 target-present and 50 target-absent scenes selected randomly from the 912 experimental images and excluded from all other analyses. Figure 4 shows maps of the best and worst predictions of the saliency model on our stimuli set.

## Guidance by target features

To date, the most well-studied sources of search guidance are target features (for reviews, see Wolfe, 2007; Zelinsky, 2008). Identifying the relevant features of an object's appearance remains a difficult issue, although recent computer vision approaches have reached excellent performance for some object classes (i.e., faces, Ullman, Vidal-Naquet, & Sali, 2002; cars, Papageorgiou & Poggio, 2000; pedestrians, Dalal & Triggs, 2005; cars, bicycles, and pedestrians, Serre, Wolf, Bileschi, Riesenhuber, & Poggio, 2007; Torralba, Fergus, & Freeman, 2008). Here, we used the person detector developed by Dalal and Triggs (2005) and Dalal, Triggs, and Schmid (2006) to model target features, as their code is available online[4] and gives state of the art detection performance at a reasonable speed.

*Implementation of the DT person detector.* The Dalal andTriggs (DT) detector is a classifier-based detector that uses a scanning window approach to explore the image at all locations and scales. The classifier extracts a set of features from each window and applies a linear Support Vector Machine (SVM) to classify the window as belonging to the target or background classes. The features are a grid of Histograms of Oriented Gradients (HOG) descriptors. The detector is sensitive to the gross structure of an upright human figure but relatively tolerant to variation in the pose of the arms and legs. We trained various implementations of the DT detector with different training set sizes and scanning window sizes, but here we report the only the results from implementation which ultimately gave the best performance on our validation set.[5] This implementation used a scanning window of $32 \times 64$ pixels and was trained on 2000 upright, unoccluded pedestrians, along with their left–right reflections. Pedestrians were cropped from images in the LabelMe database (Russell, Torralba, Murphy, & Freeman, 2008) and reduced in size to fill three-quarters of the height of the detection window. Negative training examples consisted of 30 randomly selected $32 \times 64$ pixel patches from 2000 images of outdoor scenes which did not contain people. None of the experimental stimuli were used as training images. The training process was as described in Dalal and Triggs (2005).

[4] See people detector code at http://pascal.inrialpes.fr/soft/olt/

[5] See the authors' website for details and results from the other implementations.

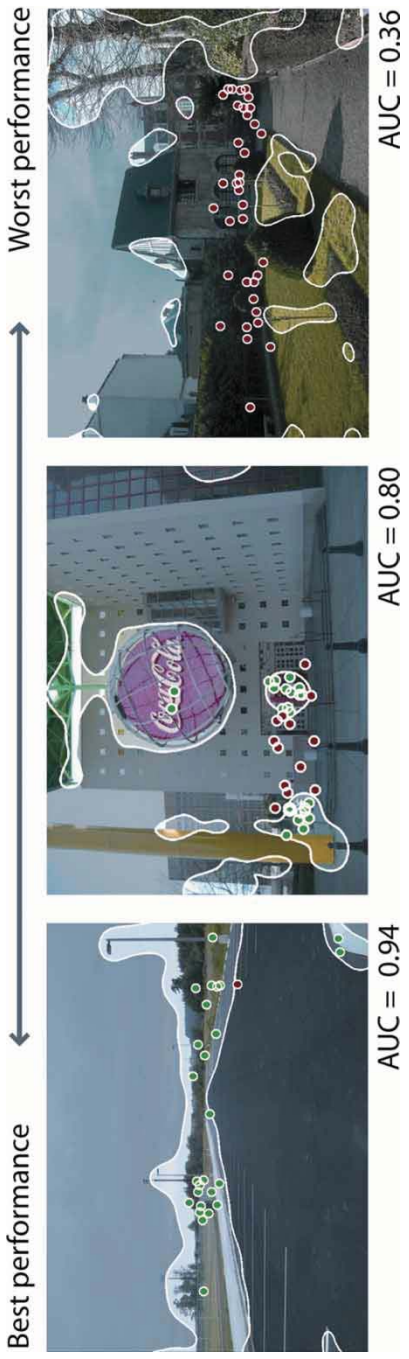


**Figure 4.** Saliency maps of the best and worst predictions on the dataset, and one mid-range image, with their AUC values. The highlighted region corresponds to 20% of the image area. Dots represent human fixations. To view this figure in colour, please see the online issue of the Journal.

The detector was tested on our stimuli set with cropped, resized pedestrians from our target-present scenes serving as positive test examples and $32 \times 64$ pixel windows from our target-absent scenes serving as negative test examples. Figure 5 shows the detection performance of our selected DT model implementation.[6] This implementation gave over 90% correct detections at a false positive rate of 10%, confirming the reliability of the DT detector on our database. Although this performance might be considered low given the exceptional performance of the DT detector on other image sets, the scenes used for our search task were particularly challenging: Targets were small, often occluded, and embedded in high

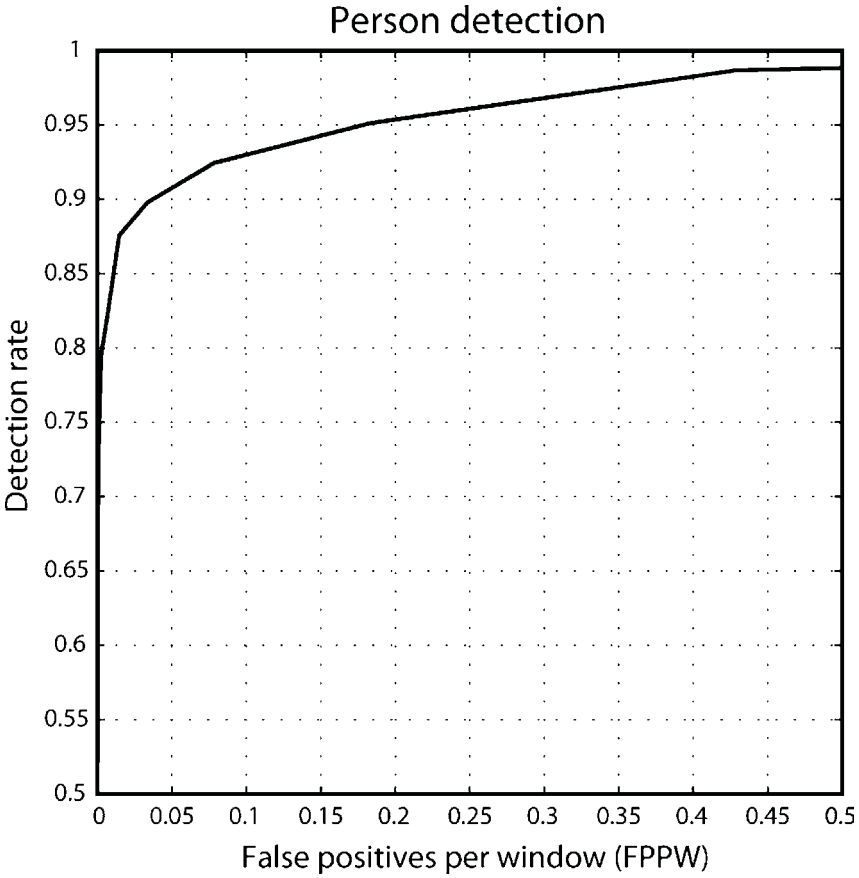


**Figure 5.** The ROC curve of the best implementation of the DT pedestrian detector, tested on our stimuli set. To view this figure in colour, please see the online issue of the Journal.

[6] See the authors' website for the detection curves of the other model implementations.

clutter. It is worth nothing that our goal was not to detect target-people in the dataset, but to use a reliable object detector as a *predictor* of human search fixations.

*Target features map.* To generate target features maps for each image, the detector was run using a sliding window that moved across the image in steps of eight pixels. Multiscale detection was achieved by iteratively reducing the image by 20% and rerunning the sliding window detector; this process was repeated until the image height was less than the height of the detector window (see Dalal & Triggs, 2005, for details). This meant that each pixel was involved in many detection windows, and therefore the detector returned many values for each pixel. We created the object detector map ($M_T$) by assigning to each pixel the highest detection score returned for that pixel (from any detection window at any scale). As with the saliency map, the resulting object detector map was raised to an exponent (.025, determined by iteratively varying the exponent to obtain the best performance on the validation set) and then blurred by applying a Gaussian filter with 50% cutoff frequency at 8 cycles/image. Figure 6 shows maps of the best and worst predictions of the target features model on our stimuli set.



## Guidance by scene context features

A mandatory role of scene context in object detection and search has been acknowledged for decades (for reviews, Bar, 2004; Chun, 2003; Oliva & Torralba, 2007). However, formal models of scene context guidance face the same problem as models of object appearance: They require knowledge about how humans represent visual scenes. Several models of scene recognition have been proposed in recent years (Bosch, Zisserman, & Muñoz, 2008; Fei Fei & Perona, 2005; Grossberg, & Huang, 2009; Lazebnik, Schmidt, & Ponce, 2006; Oliva & Torralba, 2001; Renninger & Malik, 2004; Vogel & Schiele, 2007), with most of the approaches summarizing an image's "global" features by pooling responses from low-level filters at multiple scales and orientations sampled over regions in the image.

Our model of scene context implements a top-down constraint that selects "relevant" image regions for a search task. Top-down constraints in a people-search task, for example, would select regions corresponding to sidewalks but not sky or trees. As in Oliva and Torralba (2001), we adopted a representation of the image using a set of "global features" that provide a holistic description of the spatial organization of spatial frequencies and orientations in the image. The implementation was identical to the description in Torralba et al. (2006), with the exception that the scene context model incorporated a finer spatial analysis (i.e., an $8 \times 8$ grid of

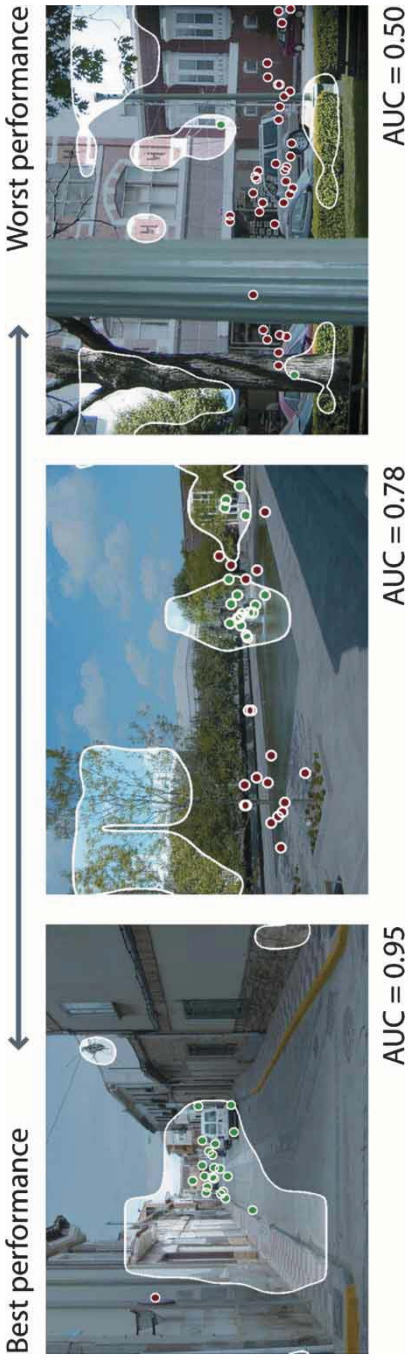


**Figure 6.** Target features maps (thresholded at 20% of the image area). Dots represent human fixations. To view this figure in colour, please see the online issue of the Journal.

nonoverlapping windows) and was trained on more images (1880 images). From each training image, we produced 10 random crops of 320 × 240 pixels to generate a training set with a uniform distribution of target locations. As in Torralba et al., the model learned the associations between the global features of an image and the location of the target. The trained computational context model compared the global scene features of a *novel* image with learned global scene features to predict the image region most highly associated with the presence of a pedestrian. This region is represented by a horizontal line at the height predicted by the model. Figure 7 shows maps of the best and worst predictions of the scene context model on our stimuli set.

There are cases of the scene context model failing to predict human fixations simply because it selected the wrong region (see Figures 7 and 8). In these cases, it would be interesting to see whether performance could be improved by a "context oracle", in which the true context region is known. It is possible to approximate contextual "ground truth" for an image by asking observers to indicate the best possible context region in each scene (Droll & Eckstein, 2008). With this information, we can establish an upper bound on the performance of a model based solely on scene context.



*Evaluating the ground truth of scene context: A "context oracle".* Seven new participants marked the context region for pedestrians in each scene in the database. The instructions were to imagine pedestrians in the most plausible places in the scene and to position a horizontal bar at the height where the heads would be. Participants were encouraged to use cues such as the horizon, the heights of doorways, and the heights of cars and signs in order to make the most accurate estimate of human head height. Image presentation was randomized and self-paced. Each participant's results served as an individual "context model", which identified the contextually relevant location for a pedestrian for each scene. The "context oracle" was created by pooling responses from all observers. Context oracle maps (Figure 8), were created by applying a Gaussian blur to the horizontal line selected by each observer, and then summing the maps produced by all participants.

## Guidance by a combined model of attention

The three models were combined by multiplying the weighted maps as shown in Equation 1. The weights ($\gamma 1 = 0.1,\ \gamma 2 = 0.85,\ \gamma 3 = 0.05$) were selected by testing various weights in the range [0,1] to find the combination which gave the best performance on the validation set. Examples of combined source model maps are shown in Figure 9.

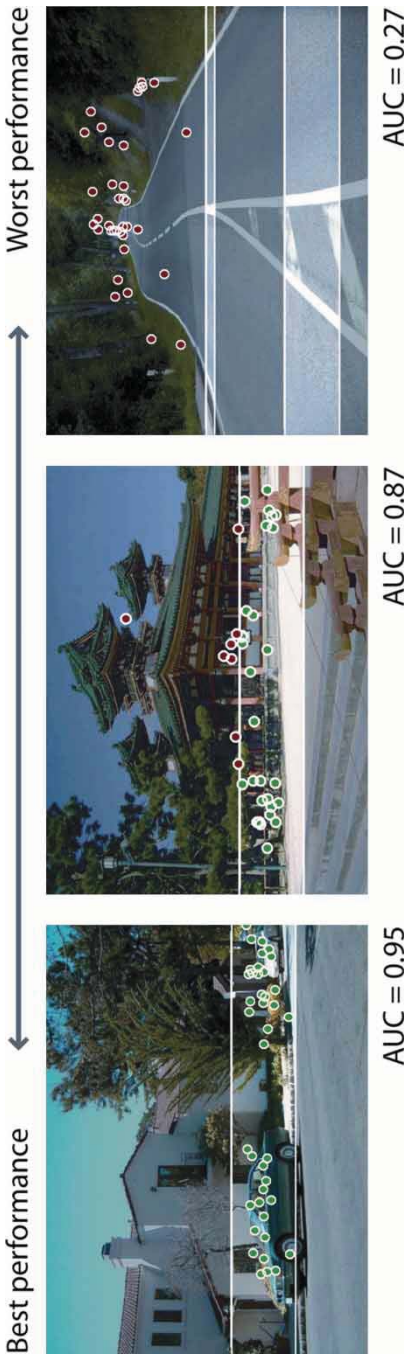


**Figure 7.** Scene context maps (thresholded at 20% of the image area). Dots represent human fixations. To view this figure in colour, please see the online issue of the Journal.

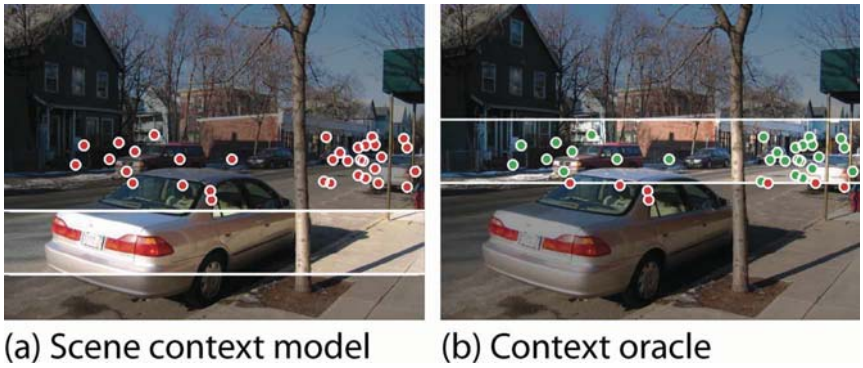


**Figure 8.** Comparison between (a) the computationally defined scene context map and (b) the empirically defined context oracle map for a single image (maps are thresholded at 20% of the image area; dots represent fixations). To view this figure in colour, please see the online issue of the Journal.



## MODELLING RESULTS

The ROC curves for all models are shown in Figure 10 and the performances are given in Table 1. Averaging across target-absent and target-present scenes, the scene context model predicted fixated regions with greater accuracy (AUC = .845) than models of saliency (.795) or target features (.811) alone. A combination of the three sources of guidance, however, resulted in greater overall accuracy (.895) than any single source model, with the overall highest performance given by a model that integrated saliency and target features with the "context oracle" model of scene context (.899). Relative to human agreement, the purely computational combined model achieved 94% of the AUC for human agreement in both target-present and target-absent scenes. When the context oracle was substituted for the scene context model, the combined model achieved on average 96% of the AUC of human agreement.

### Saliency and target features models

The saliency model had the lowest overall performance, with an AUC of .77 and .82 in target-absent and target-present scenes. This performance is within the range of values given by other saliency models predicting fixations in free viewing tasks (AUC of .727 for Itti et al., 1998; .767 for Bruce & Tsotsos, 2006; see also Harel et al., 2006).

The best example shown in Figure 4 is typical of the type of scene in which the saliency model performs very well. The saliency model does best in scenes with large homogenous regions (sky, road), and in which most of the

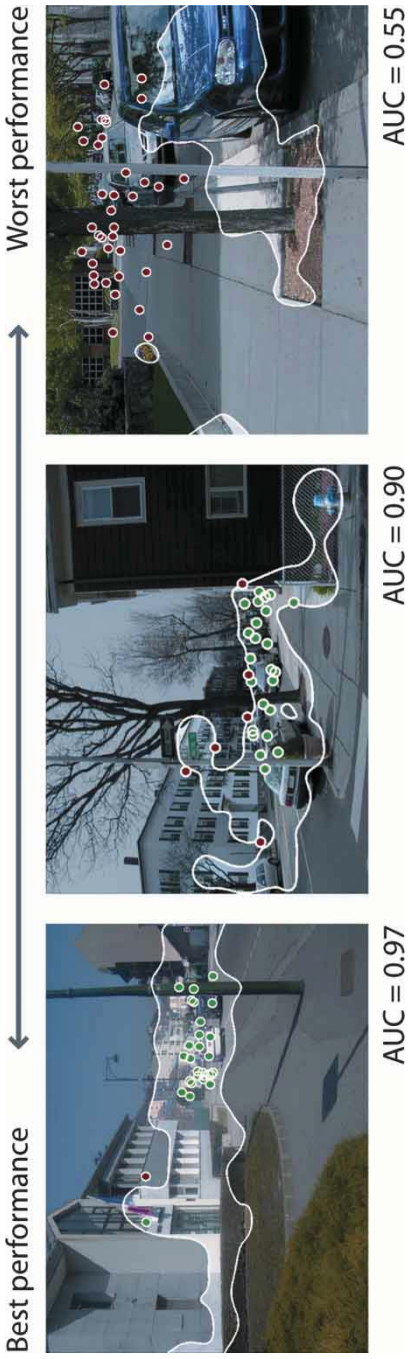


**Figure 9.** Combined source maps (thresholded at 20% of the image area). Dots represent human fixations. To view this figure in colour, please see the online issue of the Journal.

TABLE 1
Summary of performance of human observers, single source models, and combined source of guidance models

| | *Area under curve* | *Performance at 20% threshold* | *Performance at 10% threshold* |
|---|---|---|---|
| Target-absent scenes | | | |
| Human agreement | .930 | .923 | .775 |
| Cross-image control | .683 | .404 | .217 |
| Saliency model | .773 | .558 | .342 |
| Target features model | .778 | .539 | .313 |
| Scene context model | .845 | .738 | .448 |
| Context oracle | .881 | .842 | .547 |
| Saliency × Target features | .814 | .633 | .399 |
| Context × Saliency | .876 | .801 | .570 |
| Context × Target features | .861 | .784 | .493 |
| Combined source model | .877 | .804 | .574 |
| Combined model, using context oracle | .893 | .852 | .605 |
| Target-present scenes | | | |
| Human agreement | .955 | .952 | .880 |
| Cross-image control | .622 | .346 | .186 |
| Saliency model | .818 | .658 | .454 |
| Target features model | .845 | .697 | .515 |
| Scene context model | .844 | .727 | .451 |
| Context oracle | .889 | .867 | .562 |
| Saliency × Target features | .872 | .773 | .586 |
| Context × Saliency | .894 | .840 | .621 |
| Context × Target features | .890 | .824 | .606 |
| Combined source model | .896 | .845 | .629 |
| Combined model, using context oracle | .906 | .886 | .646 |



salient features coincide with the region where observers might reasonably expect to find the target. This illustrates the difficulty in determining how saliency influences eye movement guidance: In many cases, the salient regions of a real world scene are also the most contextually relevant regions. In fact, recent studies suggest that the correlation between saliency and observer's fixation selection may be an artefact of correlations between salience and higher level information (Einhauser et al., 2008; Foulsham & Underwood, 2008; Henderson et al., 2007; Stirk & Underwood, 2007; Tatler,

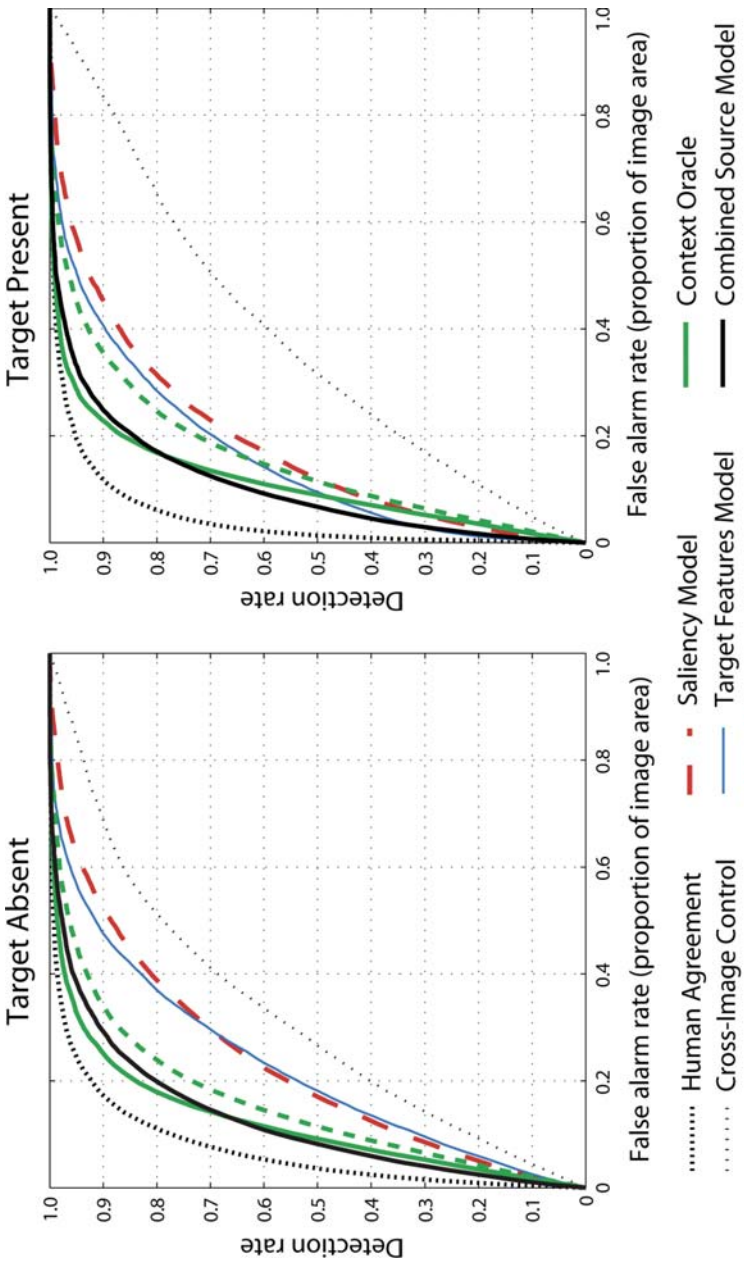


**Figure 10.** ROC curves for models. The ROC curves for human agreement and cross-image control correspond respectively to the upper and lower bounds of performance against which models were compared. To view this figure in colour, please see the online issue of the Journal.

2007). The saliency model can also give very poor predictions of human fixations in some scenes, as shown by the example in Figure 4. In a search task, saliency alone is a rather unreliable source of guidance because saliency is often created by an accidental feature (such as a reflection or a differently coloured gap between two objects) that does not necessarily correspond to an informative region.

In target-present scenes, not surprisingly, the target features model (AUC = .85) performed significantly better than the saliency model, $t(404) = 4.753$, $p < .001$. In target-absent scenes, however, the target features model (AUC = .78) did not perform significantly above the saliency model, $t(405) < 1$. Interestingly, both models were significantly correlated with each other, $r = .37$, $p < .001$, suggesting that scenes for which the saliency model was able to predict fixations well tended to be scenes in which the target features model also predicted fixations well.

Figure 5 shows target-absent images for which the target features model gave the best and worst predictions. Similar to the saliency model, the target features model tended to perform best when most of the objects were concentrated within the contextually relevant region for a pedestrian. Also like the saliency model, the target features model performed poorly when it selected accidental, nonobject features of the image (such as tree branches that happened to overlap in a vaguely human-like shape). It is important to note that the performance of the target features model is not due solely to fixations on the target. In the target-absent scenes, there was no target to find, yet the target features model was still able to predict human fixations significantly above the level of the cross-image control. Even in target-present scenes, replacing predictions of the target features model with the *true* location of the target (a "target oracle") did not explain the target model's performance on this dataset.[7]



## Context models

Overall, scene context was the most accurate single source of guidance in this search task. The computational model of scene context predicted fixation locations with an AUC of .85 and .84 in target-absent and target-present scenes, respectively. The scene context model performed significantly better than the target features model in target-absent scenes, $t(405) = 11.122$, $p < .001$, although the two models did not significantly differ in target-present scenes, $t(404) < 1$.

[7] See the authors' website for a comparison of the ROC curves of the target features model and the target oracle.

In the majority of our scenes, the computational scene context model gave a very good approximation of the location of search fixations. The first and second images in Figure 7 show the model's best and median performance, respectively, for target-absent scenes. In fact, the context model failed to predict fixated regions (i.e., had an AUC below the mean AUC of the cross-image control) in only 26 target-absent scenes and 24 target-present scenes. Typical failures are shown in Figures 7 and 8: In a few scenes, the model incorrectly identifies the relationship between scene layout and probable target location. In order to get around this problem and get a sense of the true predictive power of a context-only model of search guidance, we used the "context oracle". The empirically determined context oracle should be able to distinguish between cases in which the context model fails because it fails to identify the appropriate context region, and cases in which it fails because human fixations were largely outside the context region.

Overall performance of the context oracle was .88 and .89 for target-absent and target-present images, respectively. The context oracle performed significantly better than the computational model of scene context in target-absent, $t(405) = 8.265$, $p < .001$, and target-present, $t(404) = 8.861$, $p < .001$, scenes. Unlike any of the computational models, the context oracle performed above chance on all images of the dataset; at worst, it performed at about the level of the average AUC for the cross-image control (.68 for target-absent scenes). Examples of these failures are shown in Figure 11.

## Combined source models

A combined source model that integrated saliency, target features, and scene context outperformed all of the single source models, with an overall AUC of .88 in target-absent scenes and .90 in target-present scenes (see Table 1). The combined guidance model performed better than the best single source model (scene context) in both target-absent, $t(405) = 10.450$, $p < .001$, and target-present, $t(404) = 13.501$, $p < .001$, scenes.

Across the image set, performance of the combined model was strongly correlated with that of the scene context model, $r = .80$, $p < .001$ in target-absent scenes. The combined model was also moderately correlated with the saliency model, $r = .51$, $p < .001$ in target-absent scenes, and the target features model correlated weakly, $r = .25$, $p < .001$ in target-absent scenes. Taken together, this suggests that the success or failure of the combined model depended largely on the success or failure of its scene context component, and less on the other two components.

In order to analyse the combined model in greater detail, we also tested partial models that were missing one of the three sources of guidance (see Table 1). Removing the saliency component of the combined model

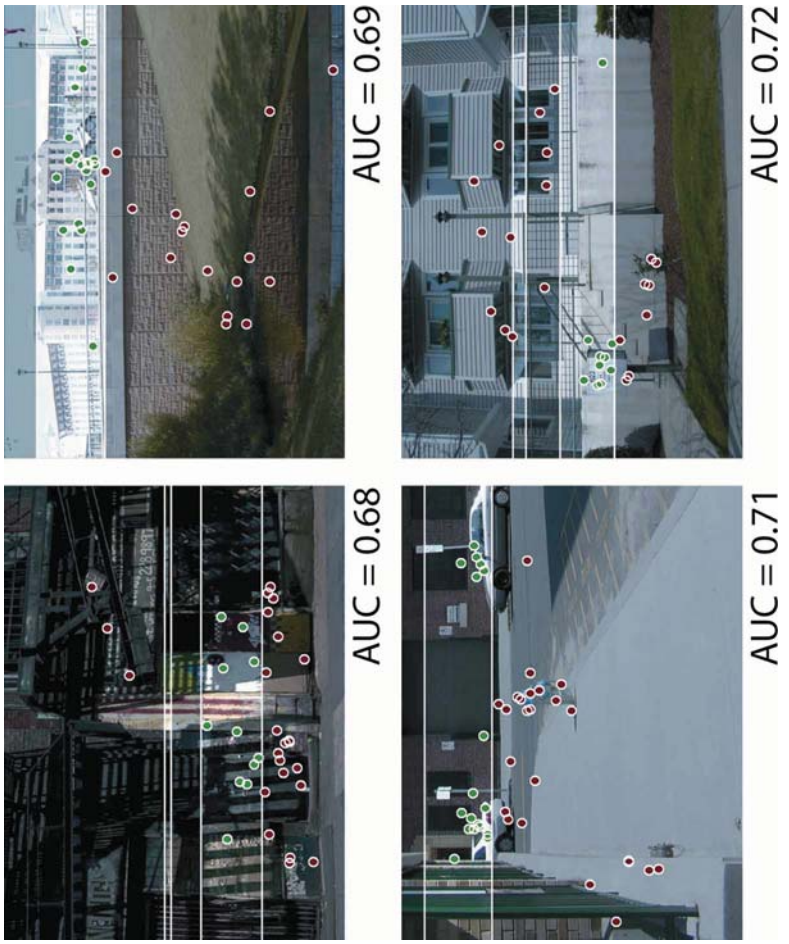


**Figure 11.** Target-absent scenes on which the context oracle performed the worst, with their corresponding AUC values. Maps are thresholded at 20% of the image area; dots represent fixations. To view this figure in colour, please see the online issue of the Journal.

produced a small but significant drop in performance in target-absent, $t(405) = 6.922$, $p < .001$, and target-present, $t(404) = 2.668$, $p < .01$, scenes. Likewise, removing the target features component of the model also produced a small but significant drop in performance in target-absent, $t(405) = 5.440$, $p < .001$, and target-present, $t(404) = 10.980$, $p < .001$, scenes. The high significance value of these extremely small drops in performance is somewhat deceptive; the reasons for this are addressed in the Discussion. Notably, the largest drop in performance resulted when the scene context component was removed from the combined model: target-absent, $t(405) = 17.381$, $p < .001$; target-present, $t(404) = 6.759$, $p < .001$.

Interestingly, the combined source model performed very similarly to the empirically defined context oracle. The difference between these two models was not significant in target-absent, $t(405) = -1.233$, $p = .218$, or target-present, $t(404) = 2.346$, $p = .019$, scenes.

Finally, the high performance of the context oracle motivated us to substitute it for the scene context component of the combined model, to see whether performance could be boosted even further. Indeed, substituting the context oracle for computational scene context improved performance in both target-absent, $t(405) = 5.565$, $p < .001$, and target-present, $t(404) = 3.461$, $p = .001$, scenes. The resulting hybrid model was almost entirely driven by the context oracle, as suggested by its very high correlation with the context oracle, $r = .97$, $p < .001$ in target-absent scenes.



## DISCUSSION

We assembled a large dataset of 912 real world scenes and recorded eye movements from observers performing a visual search task. The scene regions fixated were very consistent across different observers, regardless of whether the target was present or absent in the scene. Motivated by the regularity of search behaviour, we implemented computational models for several proposed methods of search guidance and evaluated how well these models predicted observers' fixation locations. On the target-absent scenes of the dataset, the scene context model generated better predictions (it was the best single map in 276 out of the 406 scenes) than saliency (71 scenes) or target features (59 scenes) models. Even in target-present scenes, scene context provided better predictions (191 of 405 scenes) than saliency (72 scenes) but only slightly more than target features (142 scenes). Ultimately, combining models of attentional guidance predicted 94% of human agreement, with the scene context component providing the most explanatory power.

Although the combined model is reasonably accurate at predicting human fixations, there is still room for improvement. Moving forward, even small improvements in model specificity will represent a significant

achievement. Our data shows that human observers are reasonable predictors of fixations even as map selectivity increases: 94% and 83% accuracy for selected region sizes of 20% and 10%, respectively. In contrast, the accuracy of all models fell off drastically as map selectivity increased and a region size of roughly 40% is needed for the combined model to achieve the same detection rate as human observers. Figure 12 illustrates this gap between the best computational model and human performance: Observers' fixations are tightly clustered in very specific regions, but the model selects a much more general region containing many nonfixated objects. In the following, we offer several approaches that may contribute to an improved representation of search guidance in real world scenes.

In our work, a "context region" is operationally defined as an association between certain scene regions and the presence of a target. Under this definition, a context region can be specified for any class of target and modelled using many representations. In this study, our model of scene context generated predictions based on a learned association between a representation of global image statistics and the location of a person in the scene. Compared to a model of image saliency or a model of target-like features, we found that a scene context model was better able to predict the region where people would look, regardless of whether the target was present in the scene. Moreover, the high overall accuracy of a *computational* combined source model was matched by an *empirically* derived context oracle, created by an independent set of participants marking the region which they deemed most likely to contain the target. In target-absent scenes, there was a substantial correlation between the context oracle and human agreement, $r = .54$, $p < .001$, and also between the context oracle and the combined model, $r = .50$, $p < .001$. This suggests that examining failures of the context oracle may hint at ways in which the combined model's representation fails to match human search patterns.

Figure 11 shows the worst performance of the context oracle for target-absent scenes. Why was contextual guidance insufficient for predicting the fixated regions of these scenes? One reason may be that our model of the context region did not adequately represent the real context region in certain complex scenes. We modelled the context region as a single height in the image plane, which is appropriate for most images (typically pedestrians appear on the ground plane and nowhere else). However, when the scenes contain multiple surfaces (such as balconies, ramps, and stairs) at different heights, the simplified model tends to fail. Improving the implementation of scene context to reflect that observers have expectations associated with multiple scene regions may reduce the discrepancy between model predictions and where observers look.

In addition, observers may be guided by contextual information beyond what is represented here. It is important to note that scene context can be

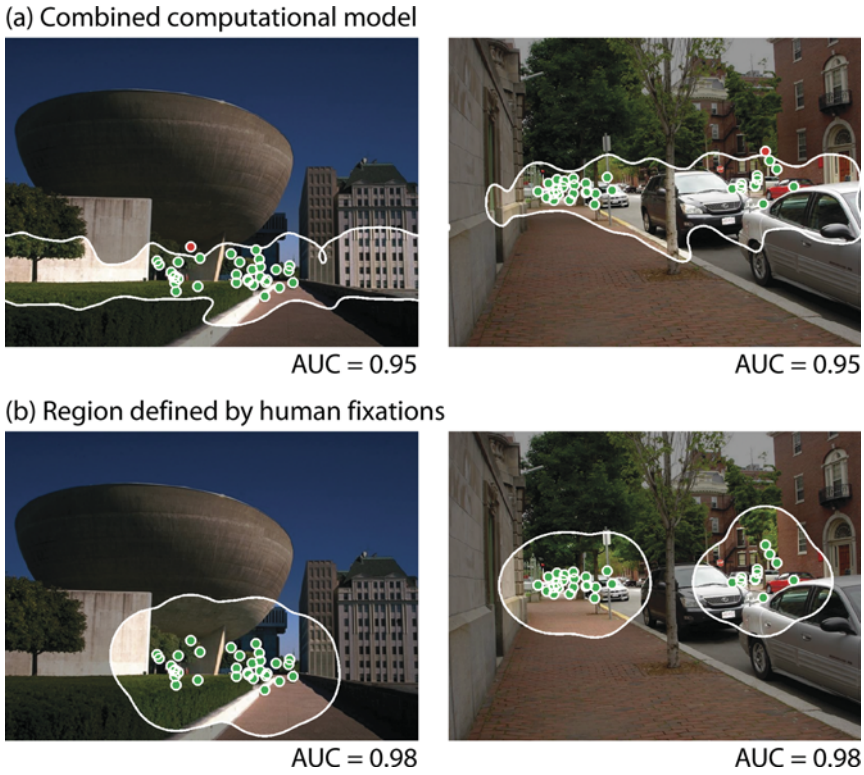


**Figure 12.** Illustration of the discrepancy between regions selected by (a) the combined computational model and (b) human fixations. To view this figure in colour, please see the online issue of the Journal.



represented with a number of approaches. Associations between the target and other *objects* in the scene, for example, may also contribute to search guidance (Kumar & Hebert, 2005; Rabinovich, Vedaldi, Galleguillos, Wiewiora, & Belongie, 2007; Torralba, Murphy, & Freeman, 2005, 2007). In our search task, for example, the presence of a person may be more strongly associated with a doorway than a garbage can. The role of semantic influences in search guidance remains an interesting and open question. Zelinsky and Schmidt (this issue 2009) explore an intermediate between search of semantically meaningful scenes and search in which observers lack expectations of target location. They find evidence that scene segmentation and flexible semantic cues can be used very rapidly to bias search to regions associated with the target (see also Eckstein et al., 2006; Neider & Zelinsky, 2006).

Scene context seems to provide the most accurate predictions in this task, which provokes the question: Is scene context *typically* the dominant source of guidance in real world search tasks? Similarly, how well do the findings of this study generalize to search for other object classes? Our search task may be biased towards context-guided search in the following ways. First, observers may have been biased to adopt a context-based strategy rather than relying on target features simply because the target pedestrians were generally very small (less than 1% of image area) and often occluded, so a search strategy based mainly on target features might have produced more false alarms than detections. Second, the large database tested here represented both semantically-consistent associations (pedestrians were supported by surfaces; Biederman et al., 1982) and location-consistent associations (pedestrians were located on *ground* surfaces). As a result, even when the target was absent from the scene, viewers expected to find their target within the context region, and therefore the scene context model predicted fixations more effectively than the target features or saliency models. Searching scenes in which the target location violated these prior expectations (e.g., person on a cloud or rooftop) might bias the pattern of fixations such that the emphasis on each source of guidance would be different from the current model.

A fully generalizable model of search behaviour may need to incorporate flexible weights on the individual sources of search guidance. Consider the example of searching for a pen in an office. Looking for a pen from the doorway may induce strategies based on convenient object relations, such as looking first to a desk, which is both strongly associated with the target and easy to discriminate from background objects. On the other hand, looking for a pen while standing in front of the desk may encourage the use of other strategies, such as searching for pen-like features. It follows that the features of the target may vary in informativeness as an observer navigates through their environment. A counting task, for example, may enhance the importance of a target features model (see Kanan, Tong, Zhang, & Cottrell, this issue 2009). The implications for the combined source model of guidance are that, not only would the model benefit from an improved representation of target features (e.g., Zelinsky, 2008), saliency (see Kanan et al., this issue 2009), or context, but the weights themselves may need to be flexible, depending on constraints not currently modelled.

In short, there is much room for further exploration: We need to investigate a variety of natural scene search tasks in order to fully understand the sources of guidance that drive attention and how they interact. It is important to acknowledge that we have chosen to implement only one of several possible representations of image saliency, target features, or scene context. Therefore, performance of the individual guidance models discussed in this paper may vary with different computational approaches. Our aim,

nevertheless, is to set a performance benchmark for how accurately a model representing combined sources of guidance can predict where human observers will fixate during natural search tasks.

## CONCLUDING REMARKS

We present a model of search guidance that combines saliency, target features, and scene context, and accounts for 94% of the agreement between human observers searching for targets in over 900 scenes. In this people-search task, the scene context model proves to be the single most important component driving the high performance of the combined source model. None of the models, however, fully capture the selectivity of the observer-defined attentional map. A comprehensive understanding of search behaviour may require that future models capture mechanisms that underlie the tight clustering of search fixations.



## REFERENCES

Andrews, T. J., & Coppola, D. M. (1999). Idiosyncratic characteristics of saccadic eye movements when viewing different visual environments. *Vision Research*, *39*, 2947–2953.

Araujo, C., Kowler, E., & Pavel, M. (2001). Eye movements during visual search: The cost of choosing the optimal path. *Vision Research*, *41*, 3613–3625.

Bar, M. (2004). Visual objects in context. *Nature Reviews Neuroscience*, *5*, 617–629.

Biederman, I., Mezzanotte, R. J., & Rabinowitz, J. C. (1982). Scene perception: Detecting and judging objects undergoing relational violations. *Cognitive Psychology*, *14*, 143–177.

Bosch, A., Zisserman, A., & Muñoz, X. (2008). Scene classification using a hybrid generative/discriminative approach. *IEEE Transactions on Pattern Analysis and Machine Intelligence*, *30*, 712–727.

Brainard, D. H. (1997). The Psychophysics Toolbox. *Spatial Vision*, *10*, 433–436.

Bravo, M. J., & Farid, H. (2006). Object recognition in dense clutter. *Perception & Psychophysics*, *68*(6), 911–918.

Bruce, N., & Tsotsos, J. K. (2006). Saliency based on information maximization. *Advances in Neural Information Processing Systems*, *18*, 155–162.

Buswell, G. T. (1935). *How people look at pictures*. Oxford, UK: Oxford University Press.

Castelhano, M. S., & Henderson, J. M. (2007). Initial scene representations facilitate eye movement guidance in visual search. *Journal of Experimental Psychology: Human Perception and Performance*, *33*, 753–763.

Chaumon, M., Drouet, V., & Tallon-Baudry, C. (2008). Unconscious associative memory affects visual processing before 100 ms. *Journal of Vision*, *8*(3), 1–10.

Chun, M. M. (2003). Scene perception and memory. In D. E. Irwin & B. H. Ross (Eds.), *The psychology of learning and motivation: Advances in research and theory* (Vol. 42, pp. 79–108). San Diego, CA: Academic Press.

Dalal, N., & Triggs, B. (2005). Histograms of oriented gradients for human detection. *IEEE Conference on Computer Vision and Pattern Recognition*, *2*, 886–893.

Dalal, N., Triggs, B., & Schmid, C. (2006). Human detection using oriented histograms of flow and appearance. *European Conference on Computer Vision*, *2*, 428–441.

De Graef, P., Christiaens, D., & d'Ydewalle, G. (1990). Perceptual effects of scene context on object identification. *Psychological Research*, *52*, 317–329.

Droll, J., & Eckstein, M. (2008). Expected object position of two hundred fifty observers predicts first fixations of seventy seven separate observers during search. *Journal of Vision*, *8*(6), 320.

Eckstein, M. P., Drescher, B. A., & Shimozaki, S. S. (2006). Attentional cues in real scenes, saccadic targeting and Bayesian priors. *Psychological Science*, *17*, 973–980.

Einhäuser, W., Rutishauser, U., & Koch, C. (2008). Task-demands can immediately reverse the effects of sensory-driven saliency in complex visual stimuli. *Journal of Vision*, *8*(2), 1–19.

Elazary, L., & Itti, L. (2008). Interesting objects are visually salient. *Journal of Vision*, *8*(3), 1–15.

Fei Fei, L., & Perona, P. (2005). A Bayesian hierarchical model for learning natural scene categories. *IEEE Proceedings in Computer Vision and Pattern Recognition*, *2*, 524–531.

Foulsham, T., & Underwood, G. (2008). What can saliency models predict about eye movements? Spatial and sequential aspects of fixations during encoding and recognition. *Journal of Vision*, *8*(2), 1–17.

Friedman, A. (1979). Framing pictures: The role of knowledge in automatized encoding and memory of gist. *Journal of Experimental Psychology: General*, *108*, 316–355.

Greene, M. R., & Oliva, A. (2009). Recognition of natural scenes from global properties: Seeing the forest without representing the trees. *Cognitive Psychology*, *58*(2), 137–179.

Grossberg, S., & Huang, T.-R. (2009). ARTSCENE: A neural system for natural scene classification. *Journal of Vision*, *9*, 1–19.

Harel, J., Koch, C., & Perona, P. (2006). Graph-based visual saliency. *Advances in Neural Information Processing Systems*, *19*, 545–552.

Hayhoe, M., & Ballard, D. (2005). Eye movements in natural behavior. *Trends in Cognitive Sciences*, *9*, 188–194.

Hayhoe, M., Shrivastava, A., Mruczek, R., & Pelz, J. B. (2003). Visual memory and motor planning in a natural task. *Journal of Vision*, *3*, 49–63.

Henderson, J. M., Brockmole, J. R., Castelhano, M. S., & Mack, M. (2007). Visual saliency does not account for eye movement during visual search in real-world scenes. In R. van Gompel, M. Fischer, W. Murray, & R. Hill (Eds.), *Eye movement research: Insights into mind and brain* (pp. 537–562). Oxford, UK: Elsevier.

Henderson, J. M., Weeks, P. A., Jr., & Hollingworth, A. (1999). Effects of semantic consistency on eye movements during scene viewing. *Journal of Experimental Psychology: Human Perception and Performance*, *25*, 210–228.

Hoiem, D., Efros, A. A., & Hebert, M. (2006). Putting objects in perspective. *IEEE Conference on Computer Vision and Pattern Recognition*, *2*, 2137–2144.

Itti, L., & Koch, C. (2000). A saliency-based search mechanism for overt and covert shifts of visual attention. *Vision Research*, *40*, 1489–1506.

Itti, L., Koch, C., & Niebur, E. (1998). A model of saliency-based visual attention for rapid scene analysis. *IEEE Transactions in Pattern Analysis and Machine Vision*, *20*(11), 12–54.

Joubert, O., Rousselet, G., Fize, D., & Fabre-Thorpe, M. (2007). Processing scene context: Fast categorization and object interference. *Vision Research*, *47*, 3286–3297.

Kanan, C., Tong, M. H., Zhang, L., & Cottrell, G. W. (2009). SUN: Top-down saliency using natural statistics. *Visual Cognition*, *17*(6/7), 979–1003.

Koch, C., & Ullman, S. (1985). Shifts in visual attention: Towards the underlying circuitry. *Human Neurobiology*, *4*, 219–227.

Kumar, S., & Hebert, M. (2005). A hierarchical field framework for unified context-based classification. *IEEE International Conference on Computer Vision*, *2*, 1284–1291.

Land, M. F., & Lee, D. N. (1994). Where we look when we steer. *Nature*, *369*, 742–744.

Land, M. F., & McLeod, P. (2000). From eye movements to actions: How batsmen hit the ball. *Nature Neuroscience*, *3*, 1340–1345.

Lazebnik, S., Schmidt, C., & Ponce, J. (2006). Beyond bags of features: Spatial pyramid matching for recognizing natural scene categories. *IEEE Conference on Computer Vision and Pattern Recognition*, *2*, 2169–2178.

Li, Z. (2002). A saliency map in primary visual cortex. *Trends in Cognitive Sciences*, *6*(1), 9–16.

Loftus, G. R., & Mackworth, N. H. (1978). Cognitive determinants of fixation location during picture viewing. *Journal of Experimental Psychology: Human Perception and Performance*, *4*, 565–572.

Mannan, S., Ruddock, K. H., & Wooding, D. S. (1995). Automatic control of saccadic eye movements made in visual inspection of briefly presented 2-D images. *Spatial Vision*, *9*, 363–386.

McCotter, M., Gosselin, F., Sowden, P., & Schyns, P. G. (2005). The use of visual information in natural scenes. *Visual Cognition*, *12*, 938–953.

Neider, M. B., & Zelinsky, G. J. (2006). Scene context guides eye movements during visual search. *Vision Research*, *46*, 614–621.

Oliva, A., & Torralba, A. (2001). Modeling the shape of the scene: A holistic representation of the spatial envelope. *International Journal of Computer Vision*, *42*, 145–175.

Oliva, A., & Torralba, A. (2006). Building the gist of a scene: The role of global image features in recognition. *Progress in Brain Research: Visual Perception*, *155*, 23–36.

Oliva, A., & Torralba, A. (2007). The role of context in object recognition. *Trends in Cognitive Sciences*, *11*(12), 520–527.

Papageorgiou, C., & Poggio, T. (2000). A trainable system for object detection. *International Journal of Computer Vision*, *38*(1), 15–33.

Parkhurst, D. J., Law, K., & Niebur, E. (2002). Modeling the role of salience in the allocation of overt visual attention. *Vision Research*, *42*, 107–123.

Parkhurst, D. J., & Niebur, E. (2003). Scene content selected by active vision. *Spatial Vision*, *16*(2), 125–154.

Pelli, D. G. (1997). The VideoToolbox software for visual psychophysics: Transforming numbers into movies. *Spatial Vision*, *10*, 437–442.

Peters, R. J., Iyer, A., Itti, L., & Koch, C. (2005). Components of bottom-up gaze allocation in natural images. *Vision Research*, *45*, 2397–2416.

Pomplun, M. (2006). Saccadic selectivity in complex visual search displays. *Vision Research*, *46*, 1886–1900.

Rabinovich, A., Vedaldi, A., Galleguillos, C., Wiewiora, E., & Belongie, S. (2007). Objects in context. *IEEE International Conference on Computer Vision*, 1–8.

Rao, R. P. N., Zelinsky, G., Hayhoe, M. M., & Ballard, D. H. (2002). Eye movements in iconic visual search. *Vision Research*, *42*, 1447–1463.

Renninger, L. W., & Malik, J. (2004). When is scene identification just texture recognition? *Vision Research*, *44*, 2301–2311.

Renninger, L. W., Verghese, P., & Coughlan, J. (2007). Where to look next? Eye movements reduce local uncertainty. *Journal of Vision*, *7*(3), 1–17.

Rodriguez-Sanchez, A. J., Simine, E., & Tsotsos, J. K. (2007). Attention and visual search. *International Journal of Neural Systems*, *17*(4), 275–288.

Rosenholtz, R. (1999). A simple saliency model predicts a number of motion popout phenomena. *Vision Research*, *39*, 3157–3163.

Rosenholtz, R., Li, Y., & Nakano, L. (2007). Measuring visual clutter. *Journal of Vision*, *7*(2), 1–22.

Rousselet, G. A., Joubert, O. R., & Fabre-Thorpe, M. (2005). How long to get to the "gist" of real-world natural scenes? *Visual Cognition*, *12*, 852–877.

Russell, B., Torralba, A., Murphy, K., & Freeman, W. T. (2008). LabelMe: A database and web-based tool for image annotation. *International Journal of Computer Vision*, *77*, 157–173.

Schyns, P. G., & Oliva, A. (1994). From blobs to boundary edges: Evidence for time- and spatial-scale-dependent scene recognition. *Psychological Science*, *5*, 195–200.

Serre, T., Wolf, L., Bileschi, S., Riesenhuber, M., & Poggio, T. (2007). Object recognition with cortex-like mechanisms. *IEEE Transactions on Pattern Analysis and Machine Intelligence*, *29*(3), 411–426.

Stirk, J. A., & Underwood, G. (2007). Low-level visual saliency does not predict change detection in natural scenes. *Journal of Vision*, *7*(10), 1–10.

Tatler, B. W. (2007). The central fixation bias in scene viewing: Selecting an optimal viewing position independently of motor biases and image feature distributions. *Journal of Vision*, *7*(14), 1–17.

Tatler, B. W., Baddeley, R. J., & Gilchrist, I. D. (2005). Visual correlates of fixation selection: Effects of scale and time. *Vision Research*, *45*(5), 643–659.

Tatler, B. W., Baddeley, R. J., & Vincent, B. T. (2006). The long and the short of it: Spatial statistics at fixation vary with saccade amplitude and task. *Vision Research*, *46*(12), 1857–1862.

Tatler, B. W., & Vincent, B. T. (2009). The prominence of behavioural biases in eye guidance. *Visual Cognition*, *17*(6/7), 1029–1054.

Torralba, A. (2003a). Contextual priming for object detection. *International Journal of Computer Vision*, *53*(2), 169–191.

Torralba, A. (2003b). Modeling global scene factors in attention. *Journal of Optical Society of America*, *20A*(7), 1407–1418.

Torralba, A., Fergus, R., & Freeman, W. T. (2008). 80 million tiny images: A large dataset for non-parametric object and scene recognition. *IEEE Transactions on Pattern Analysis and Machine Intelligence*, *30*, 1958–1970.

Torralba, A., Murphy, K. P., & Freeman, W. T. (2005). Contextual models for object detection using boosted random fields. *Advances in Neural Information Processing Systems*, *17*, 1401–1408.

Torralba, A., Murphy, K. P., & Freeman, W. T. (2007). Sharing visual features for multiclass and multiview object detection. *IEEE Transactions on Pattern Analysis and Machine Intelligence*, *29*(5), 854–869.

Torralba, A., & Oliva, A. (2002). Depth estimation from image structure. *IEEE Pattern Analysis and Machine Intelligence*, *24*, 1226–1238.

Torralba, A., & Oliva, A. (2003). Statistics of Natural Images Categories. *Network: Computation in Neural Systems*, *14*, 391–412.

Torralba, A., Oliva, A., Castelhano, M., & Henderson, J. M. (2006). Contextual guidance of eye movements and attention in real-world scenes: The role of global features in object search. *Psychological Review*, *113*, 766–786.

Treisman, A., & Gelade, G. (1980). A feature integration theory of attention. *Cognitive Psychology*, *12*, 97–136.

Tsotsos, J. K., Culhane, S. M., Wai, W. Y. K., Lai, Y. H., Davis, N., & Nuflo, F. (1995). Modeling visual-attention via selective tuning. *Artificial Intelligence*, *78*, 507–545.

Ullman, S., Vidal-Naquet, M., & Sali, E. (2002). Visual features of intermediate complexity and their use in classification. *Nature Neuroscience*, *5*, 682–687.

Van Zoest, W., Donk, M., & Theeuwes, J. (2004). The role of stimulus-driven and goal-driven control in saccadic visual selection. *Journal of Experimental Psychology: Human Perception and Performance*, *30*, 746–759.

Vogel, J., & Schiele, B. (2007). Semantic scene modeling and retrieval for content-based image retrieval. *International Journal of Computer Vision*, *72*(2), 133–157.

Wolfe, J. M. (1994). Guided Search 2.0: A revised model of visual search. *Psychonomic Bulletin and Review*, *1*, 202–228.

Wolfe, J. M. (2007). Guided Search 4.0: Current progress with a model of visual search. In W. Gray (Ed.), *Integrated models of cognitive systems* (pp. 99–119). New York: Oxford Press.

Wolfe, J. M., Cave, K. R., & Franzel, S. L. (1989). Guided Search: An alternative to the feature integration model for visual search. *Journal of Experimental Psychology: Human Perception and Performance*, *15*, 419–433.

Wolfe, J. M., & Horowitz, T. S. (2004). What attributes guide the deployment of visual attention and how do they do it? *Nature Reviews Neuroscience*, *5*(6), 495–501.

Yarbus, A. (1967). *Eye movements and vision*. New York: Plenum Press.

Zelinsky, G. J. (2008). A theory of eye movements during target acquisition. *Psychological Review*, *115*, 787–835.

Zelinsky G. J., & Schmidt, J. (2009). An effect of referential scene constraint on search implies scene segmentation. *Visual Cognition*, *17*(6/7), 1004–1028.